ACS OMEGA

http://pubs.acs.org/journal/acsodf

Article

Antibiotic Alleviates Radiation-Induced Intestinal Injury by Remodeling Microbiota, Reducing Inflammation, and Inhibiting Fibrosis

Zhenguo Zhao, Wei Cheng, Wei Qu, Guoyi Shao,* and Shuanghai Liu*

Cite This: *ACS Omega* 2020, 5, 2967−2977

Read Online

ACCESS | Metrics & More | Article Recommendations | Supporting Information

ABSTRACT: Radiation-induced intestinal injury is a common complication of abdominal radiation therapy. However, the pathological features of radiation-induced intestinal injury and its therapeutic regimen are not very clear. The aim of this study was to investigate the effects of antibiotic pretreatment on radiation-induced intestinal injury. Abdominal radiation disrupted the intestinal microbiota balance and significantly reduced bacterial diversity in mice. Antibiotic cocktail (Abx) pretreatment effectively removed the intestinal microbiota of mice, and metronidazole also reduced the diversity of intestinal bacteria to some extent. Two antibiotic pretreatment regimens improved the reconstitution ability of the gut microbiota in mice after radiation. Further experiments showed that Abx pretreatment effectively reduced the content of lipopolysaccharide (LPS) and inhibited the TLR4/MyD88/NF-κB signaling pathway in the ileum. In addition, Abx pretreatment regulated macrophage cell polarization in the ileum, down-regulated TGF-β1, phosphorylated Smad-3 and α-SMA protein levels, and upregulated E-cadherin protein expression. Eventually, Abx pretreatment significantly improved the survival rate and attenuated intestinal injury of mice after radiation by reducing inflammation and preventing intestinal fibrosis. These results revealed that antibiotic pretreatment can effectively alleviate gut microbiota turbulence and intestinal damage caused by abdominal radiation in mice. Collectively, these findings add to our understanding of the pathogenesis of radiation enteritis.

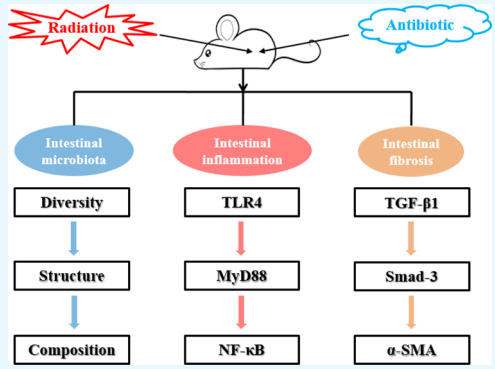

INTRODUCTION

Radiation therapy has been an important treatment for cancer patients in the past few decades. Despite advances in radiation technology, collateral damage to surrounding healthy tissues remains a major complication of radiation therapy. Abdominal radiotherapy will cause acute and chronic damage to the intestine, manifested as radiation-induced intestinal damage, clinically known as radiation enteropathy.[1,2] Although the mortality and prevalence associated with radiation-induced intestinal damage have been valued, the understanding of its pathophysiology and treatment options remains incomplete.[3]

Studies have declared that ionizing radiation can directly cause DNA damage.[4] In addition, ionizing radiation causes radiation decomposition of water and stimulates nitric oxide synthase to produce reactive oxygen species (ROS) and reactive nitrogen species (RNS), respectively. Radiation also causes electron leakage from the mitochondria, resulting in excess ROS and superoxide.[5] The toxic effects of these molecules include DNA/RNA damage, amino acid oxidation, and lipid peroxidation, resulting in intracellular nucleic acid damage, mutations, and protein and lipid damage.[6,7] Depending on the intensity of the radiation, the overall acute consequences of radiation on the intestine are tight junction integrity disruption and crypt and villus epithelial cell death.[8,9] These effects can lead to the development of inflammation and the destruction of the mucosal barrier, allowing intestinal contents, especially microorganisms, to flow into the lamina propria, triggering the recruitment of further inflammatory factors and immune cells.[10,11]

With the development of next-generation sequencing, such as 16S rRNA gene amplicon analysis, there is new evidence that the intestinal microbiota plays an important role in the pathogenesis of radiation-induced intestinal damage. Studies have shown that radiation can cause significant changes in the gut microbiota.[12,13] In addition, a previous study has shown that microbiome plays an important role in the pathogenesis of radiation-induced intestinal damage using mice as a model.[14] This study demonstrated for the first time that radiation-induced microbiota dysregulation increases intestinal susceptibility to injury. However, the mechanism by which sterile mice can resist radiation damage is unclear. Therefore, the purpose of this study is to (1) investigate the effects of abdominal

Received: November 15, 2019
Accepted: January 20, 2020
Published: February 5, 2020

https://dx.doi.org/10.1021/acsomega.9b03906
ACS Omega 2020, 5, 2967−2977

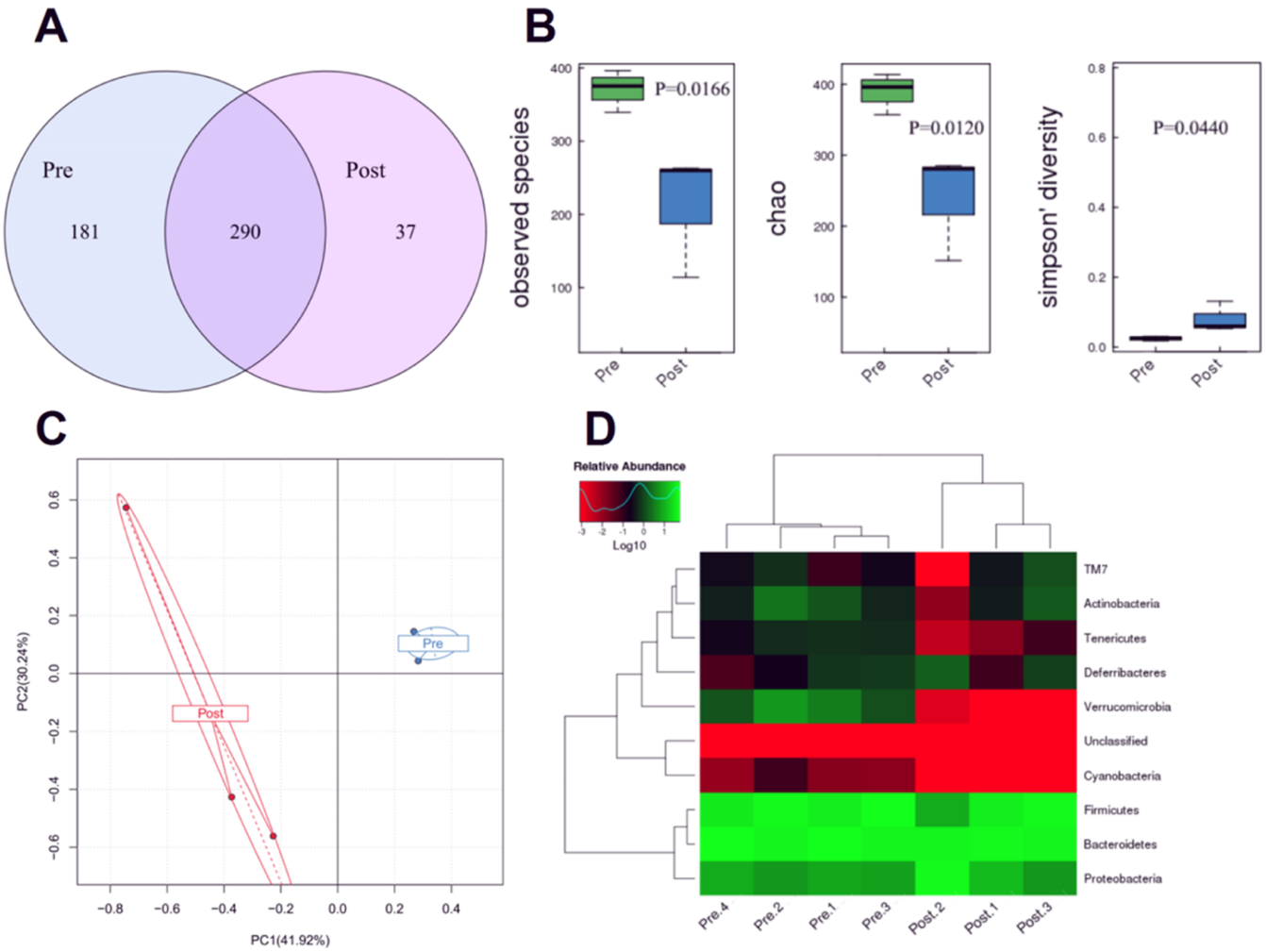

Figure 1. Abdominal radiation changes the gut microbiota of mice. (A) Venn diagram illustrating overlap of gut microbiota OTUs for pre- and postradiation groups. (B) Alpha-diversity of the gut microbiota community for Pre- and Postradiation groups. (C) PCA of gut microbiota for Pre- and Postradiation group. (D) Heat map analysis of gut microbiota for pre- and postradiation groups. The results were expressed as mean ± SEM. n = 4/3. *P < 0.05.

radiation on the intestinal microbiota of mice; (2) evaluate the effect of antibiotic pretreatment on intestinal microbiota reconstruction after radiation-induced intestinal injury; and (3) explore the protective effect of antibiotic pretreatment on radiation intestinal injury and its potential mechanism.

RESULTS

Effect of Abdominal Radiation on Gut Microbiota in Mice. There were 290 common OTUs in the preradiation (Pre.Con14 group) and postradiation (Post.Con14 group). The Pre group had 181 special OTUs, and the Post group only had 37 special OTUs (Figure 1A). As shown in Figure 1B, the observed species (represents the number of OTUs actually detected) and chao index (represents the richness of microorganisms) in the Post group were significantly lower than those of the Pre group, and the Simpson diversity index (represents the diversity of microorganisms) in the Post group was significantly greater than that of the Pre group. The principal component analysis (PCA) plot showed that the Pre group had a smaller intragroup difference, while the Post group had a larger intragroup difference (Figure 1C). From the heat map of the phylum level, the Pre group gut microbiota were mainly composed of *Bacteroidetes* (45.9%), *Firmicutes* (41.3%), *Proteobacteria* (7.4%), *Verrucomicrobia* (2.9%), and *Actinobacteria* (1.2%), while the Post group was mainly from *Bacteroidetes* (44.6%), *Firmicutes* (31.3%), *Proteobacteria* (22.0%), and *Actinobacteria* (0.6%) (Figure 1D).

Effect of Antibiotic Pretreatment on Gut Microbiota before Radiation in Mice. As shown in Figure 2A, there were only 71 common OTUs in the normal saline pretreatment group (Pre.Con14 group), metronidazole (MDE) pretreatment group (Pre.MDE14 group), and antibiotic cocktail (Abx) pretreatment group (Pre.Abx14 group); 165 special OTUs in the Pre.Con14 group; 54 special OTUs in the Pre.MDE14 group; and 12 special OTUs in the Pre.Abx14 group. Alpha-diversity analysis results display that the observed species and chao index in Pre.MDE14 and Pre.Abx14 groups were significantly lower than those of the Pre.Con14 group, and the Simpson diversity index in Pre.MDE14 and Pre.Abx14 groups was significantly greater than that of the Pre.Con14 group (Figure 2B). The PCA plot showed that the main components of the gut microbiota were changed after antibiotic pretreatment (Figure 2C). From the heat map of the phylum level, the abundance of all the microbes in the Pre.Abx14 group was significantly reduced compared to the Pre.Con14 group, whereas the Pre.MDE14 group was only

https://dx.doi.org/10.1021/acsomega.9b03906
ACS Omega 2020, 5, 2967−2977

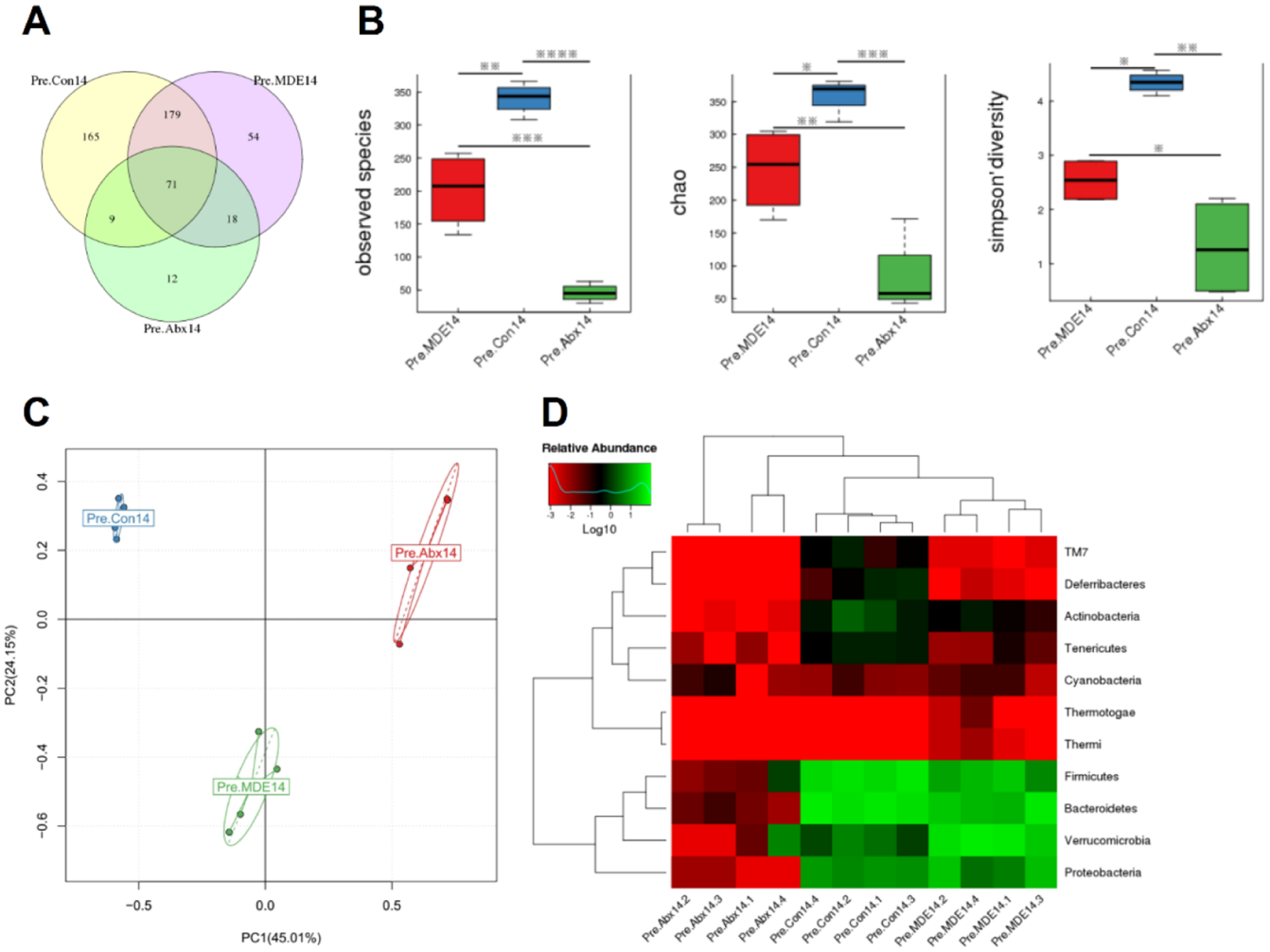

Figure 2. Antibiotic pretreatment 14d alters gut microbiota of mice (A) Venn diagram illustrating overlap of gut microbiota OTUs for Pre.Con14, Pre.MDE14, and Pre.Abx14 groups. (B) Alpha-diversity of the gut microbiota community for Pre.Con14, Pre.MDE14, and Pre.Abx14 groups. (C) PCA of gut microbiota for Pre.Con14, Pre.MDE14, and Pre.Abx14 groups. (D) Heat map analysis of gut microbiota for Pre.Con14, Pre.MDE14, and Pre.Abx14 groups. The results were expressed as mean ± SEM. $n = 4$. *$P < 0.05$.

partially reduced (Figure 2D). To make matters worse, MDE pretreatment resulted in gut dysbiosis and a large increase in Gram-negative pathogenic bacteria such as *Escherichia coli* ($P < 0.05$) and *Shigella* ($P < 0.05$), compared with Ns pretreatment.

Effect of Antibiotic Pretreatment on Reconstruction of Gut Microbiota 3 Months after Radiation. There were 254 common OTUs in the Post.Con14 group, Post.MDE14 group, and Post.Abx14 group; 21 special OTUs in the Post.Con14 group; 73 special OTUs in the Post.MDE14 group; and 44 special OTUs in the Post.Abx14 group (Figure 3A). Compared with the Post.Con14 group, the observed species and chao index in the Post.MDE14 group were significantly higher than those in the Post.Con14 group. Although the Post.Abx14 group increased alpha-diversity, there was no statistical difference (Figure 3B). The PCA plot showed that the main components of the gut microbiota of mice were different among three groups (Figure 3C). From the heat map of the phylum level, the abundance of the microbes in the Post.Abx14 group and Post.MDE14 was significantly higher than that of the Post.Con14 group (Figure 3D).

Effect of Antibiotic Pretreatment on the Survival Rate and Ileum Apoptosis and Proliferation in Mice. Compared with the normal saline pretreatment group (Ns group), the Abx group had a higher survival rate, but the MDE group could not improve the survival rate after radiation intestinal injury in mice (Figure 4). In addition, the villus height, crypt depth, and epithelium thickness of the Abx group were significantly higher than those in the Ns group and MDE group 12 h and 3 days after abdominal radiation (Figure S1). As shown in Figure 5, Abx and MDE did not affect the protein levels of PCNA and cleaved caspase3 before radiation (Figure 5A). In the chronic stage, the protein levels of PCNA and cleaved caspase3 in Abx group mice were significantly higher than those in the other two groups at 1 and 3 months after radiation (Figure 5B,C). In the acute stage, Ki67 staining results revealed that the proliferation of the Abx group is much better than those in the two other groups 12 h and 3 days after abdominal radiation (Figure S2).

Effect of Antibiotic Pretreatment on Ileal Fibrosis in Mice. As shown in Figures 6 and S3, HE, Masson, and Sirius red staining results indicated that Abx and MDE pretreatment did not affect the thickness of submucosa and collagen expression in the ileum before abdominal radiation. 1 and 3 months after abdominal radiation, the thickness of submucosa and collagen expression significantly increased in the Ns and MDE groups, whereas the Abx pretreatment significantly

https://dx.doi.org/10.1021/acsomega.9b03906
ACS Omega 2020, 5, 2967−2977

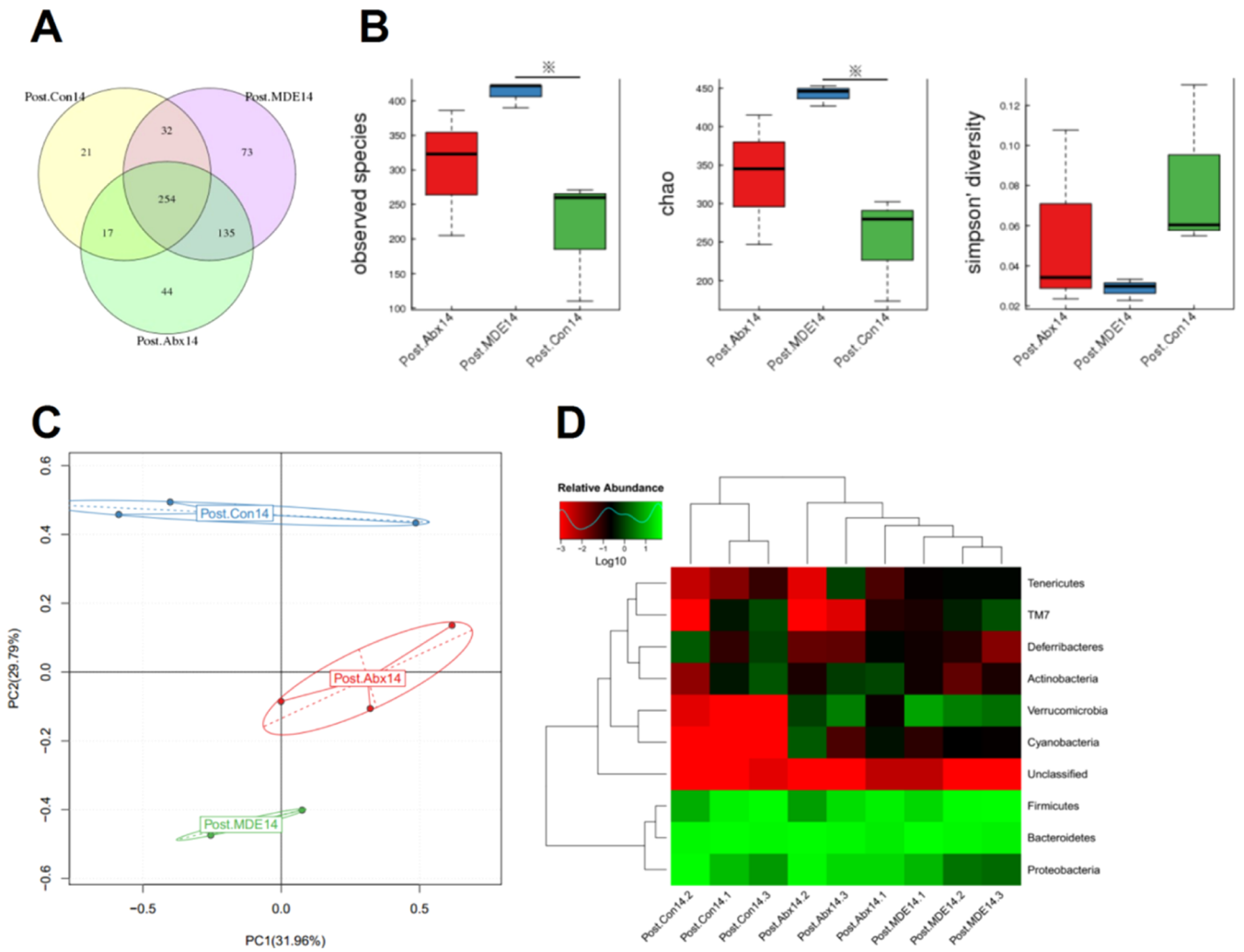

Figure 3. Antibiotic pretreatment improves reconstruction of gut microbiota after radiation for 3 months. (A) Venn diagram illustrating overlap of gut microbiota OTUs for Post.Con14, Post.MDE14, and Post.Abx14 groups. (B) Alpha-diversity of the gut microbiota community for Post.Con14, Post.MDE14, and Post.Abx14 groups. (C) PCA of gut microbiota for Post.Con14, Post.MDE14, and Post.Abx14 groups. (D) Heat map analysis of gut microbiota for Post.Con14, Post.MDE14, and Post.Abx14 groups. The results were expressed as mean ± SEM. $n = 3$. *$P < 0.05$.

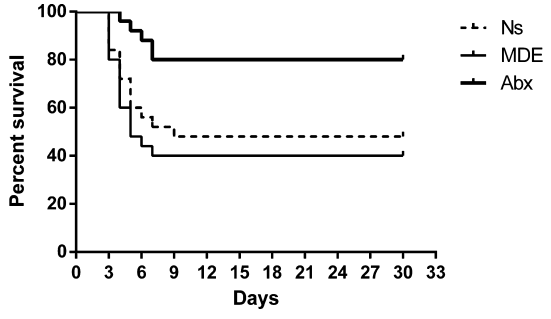

Figure 4. Antibiotic pretreatment elevates the survival rate of mice.

reduced the thickness of submucosa and collagen expression in the ileum, compared with the other two groups.

Effect of Antibiotic Pretreatment on the TLR4/MyD88/NF-κB p65 Signaling Pathway in the Ileum of Mice. Abx and MDE pretreatment (0.008, 0.008, and 0.008 pg/mL for the NS, MDE, and Abx groups, respectively) did not affect the content of LPS in ileum tissue before the mice received abdominal radiation (Figure 7A). However, 12 h (1.467, 2.126, and 0.223 pg/mL for the NS, MDE, and Abx groups, respectively) and 3 days (0.222, 0.35, and 0.127 pg/mL for the NS, MDE, and Abx groups, respectively) after the radiation, the Abx group significantly reduced the LPS content in the ileum, compared with the other two groups (Figure 7A). As shown in Figure 7B−D, Abx and MDE pretreatment did not change the protein expression of TLR4, MyD88, and phosphorylated NF-κB p65 in ileum tissue before abdominal radiation. After radiation for 12 h and 3 days, the protein abundance of TLR4, MyD88, and phosphorylated NF-κB p65 was significantly lower in the Abx group than that in Ns and MDE groups.

Effect of Antibiotic Pretreatment on iNOS and CD163 Protein Expression in the Ileum of Mice. Abx and MDE pretreatment did not affect the protein expression of iNOS and CD163 in ileum tissue before abdominal radiation (Figure 8A). The protein abundance of iNOS (M1 maker) and CD163 (M2 maker) was remarkably downregulated in the Abx group than that in Ns and MDE groups.

Effects of Antibiotic Pretreatment on the TGF-β1/Smad-3/α-SMA/E-Cadherin Signaling Pathway in the Ileum of Mice. As shown in Figure 9, the protein levels of TGF-β1, phosphorylated Smad-3, and α-SMA in the Abx

https://dx.doi.org/10.1021/acsomega.9b03906
ACS Omega 2020, 5, 2967−2977

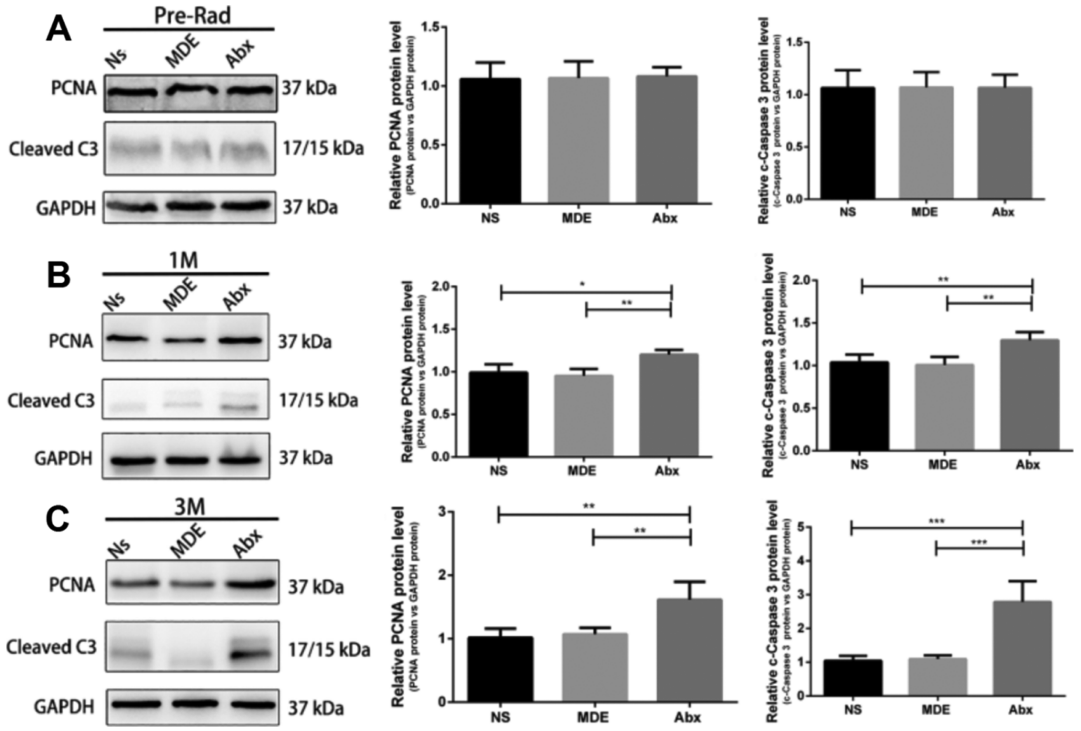

Figure 5. Antibiotic pretreatment promotes ileum apoptosis and proliferation in mice. (A) Protein expression of PCNA and cleaved caspase3 of the ileum in preradiation mice. (B) Protein expression of PCNA and cleaved caspase3 of the ileum of mice 1 month after radiation. (C) Protein expression of PCNA and cleaved caspase3 of the ileum of mice 3 months after radiation. The results were expressed as mean ± SEM. $n = 5$.*$P < 0.05$, **$P < 0.01$.

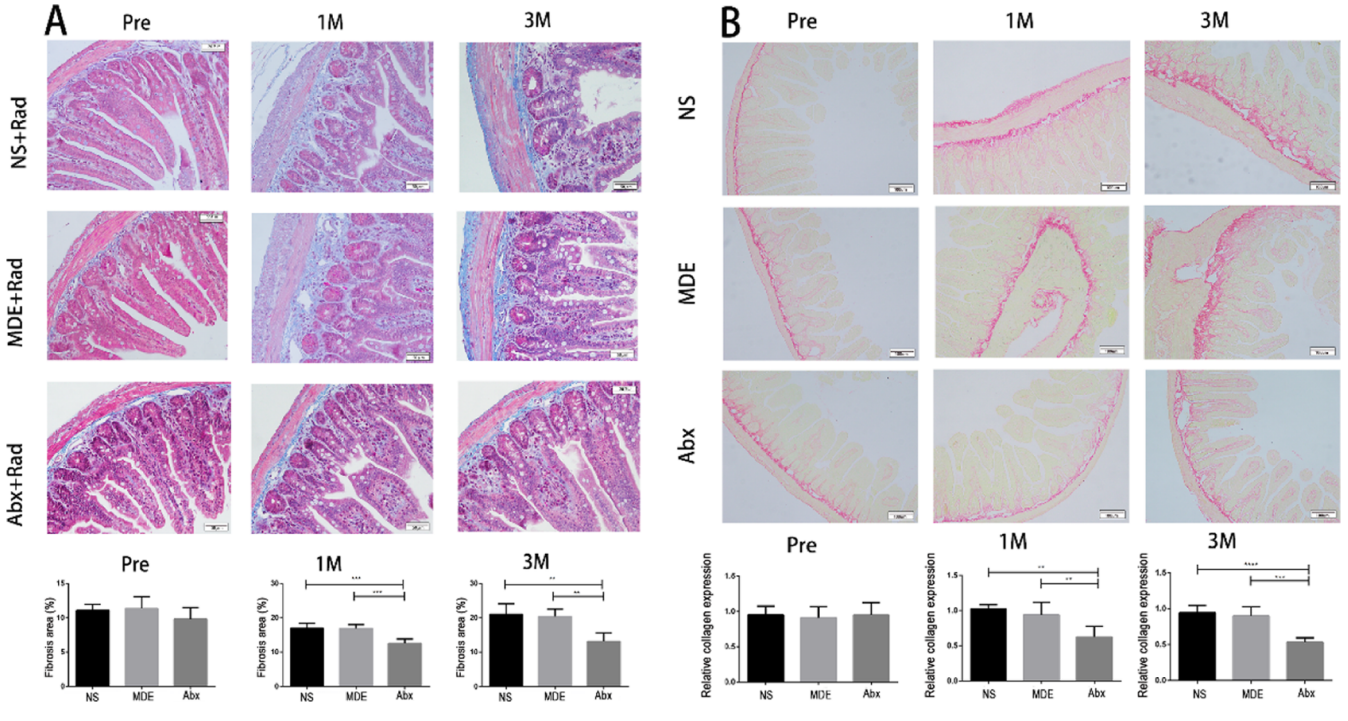

Figure 6. Antibiotic pretreatment reduces ileal fibrosis in mice. (A) Mason staining of the ileum (×100). (B) Sirius red staining of the ileum (×100). The results were expressed as mean ± SEM. $n = 5$. **$P < 0.01$, ***$P < 0.001$, ****$P < 0.0001$.

group were significantly lower than those in the Ns and MDE groups in the ileum, 1 and 3 months after radiation. In contrast, the protein abundance of Smad-3 and E-cadherin in the Abx group was significantly higher than those in Ns and MDE groups.

DISCUSSION

Radiation therapy is a commonly used method in cancer therapy, especially in the treatment of gynecological and colorectal cancer. About 60% of patients with gynecological or colorectal cancer have received radiation therapy, and about

https://dx.doi.org/10.1021/acsomega.9b03906
ACS Omega 2020, 5, 2967−2977

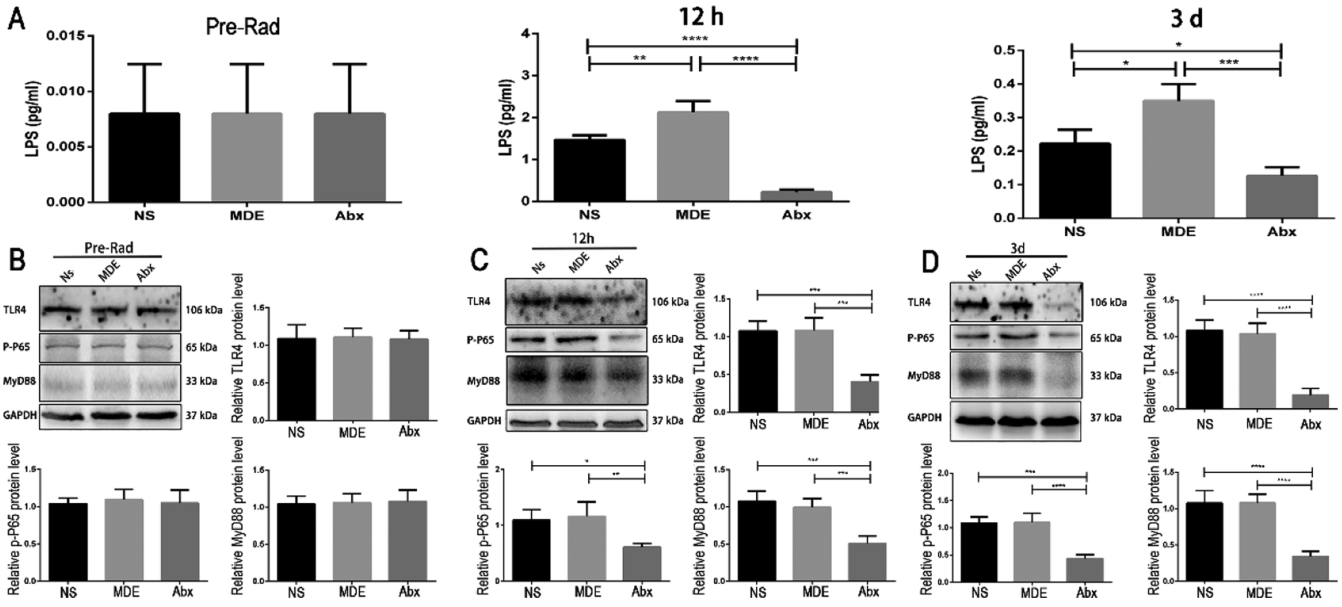

Figure 7. Antibiotic pretreatment inhibits the TLR4/MyD88/NF-κB p65 signaling pathway in the ileum of mice. (A) LPS content of the ileum of mice before radiation, 12 h after radiation, and 3d after radiation. (B) Protein expression of TLR4/MyD88/NF-κB p65 of the ileum in preradiation mice. (C) Protein expression of TLR4/MyD88/NF-κB p65 in the ileum of mice 12 h after radiation. (D) Protein expression of TLR4/MyD88/NF-κB p65 in the ileum of mice 3d after radiation. The results were expressed as mean ± SEM. $n = 5$. $^{*}P < 0.05$, $^{**}P < 0.01$, $^{***}P < 0.001$, $^{****}P < 0.0001$.

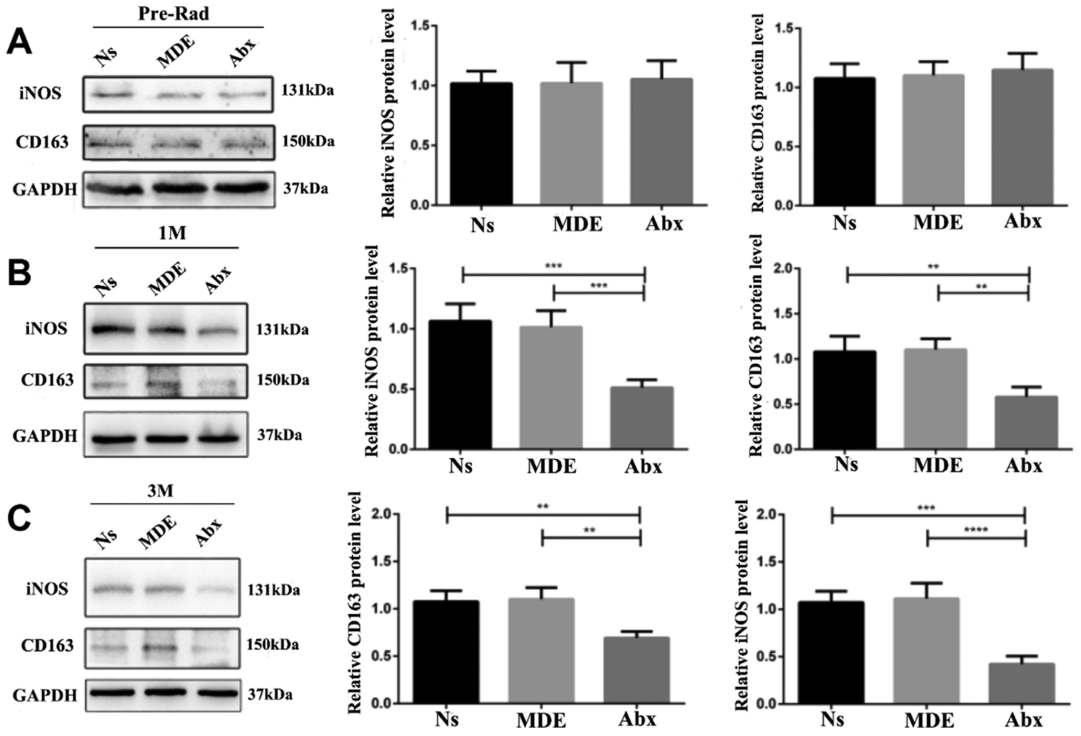

Figure 8. Antibiotic pretreatment reduces iNOS and CD163 protein expression in the ileum of mice. (A) Protein expression of iNOS and CD163 of the ileum in preradiation mice. (B) Protein expression of iNOS and CD163 in the ileum of mice 1 month after radiation. (C) Protein expression of iNOS and CD163 in the ileum of mice 3 months after radiation. The results were expressed as mean ± SEM. $n = 3$. $^{**}P < 0.01$,$^{***}P < 0.001$, $^{****}P < 0.0001$.

75% of them have symptoms of gastrointestinal discomfort caused by radiotherapy, including diarrhea, abdominal pain, malabsorption, rectal bleeding, urgency, and fecal incontinence.[15−17] In the current study, we confirmed that abdominal radiation therapy caused gut microbiota disorder and reduced alpha- and beta-diversity in mice, which was consistent with previous findings in clinical patients.[18] In addition, we systematically investigated the effect of antibiotic pretreatment on the reconstruction of gut microbiota after radiation, its protective effect on radiation-induced intestinal injury, and its potential mechanism, using microbiota analysis and molecular biology technology. Our findings showed that

https://dx.doi.org/10.1021/acsomega.9b03906
ACS Omega 2020, 5, 2967−2977

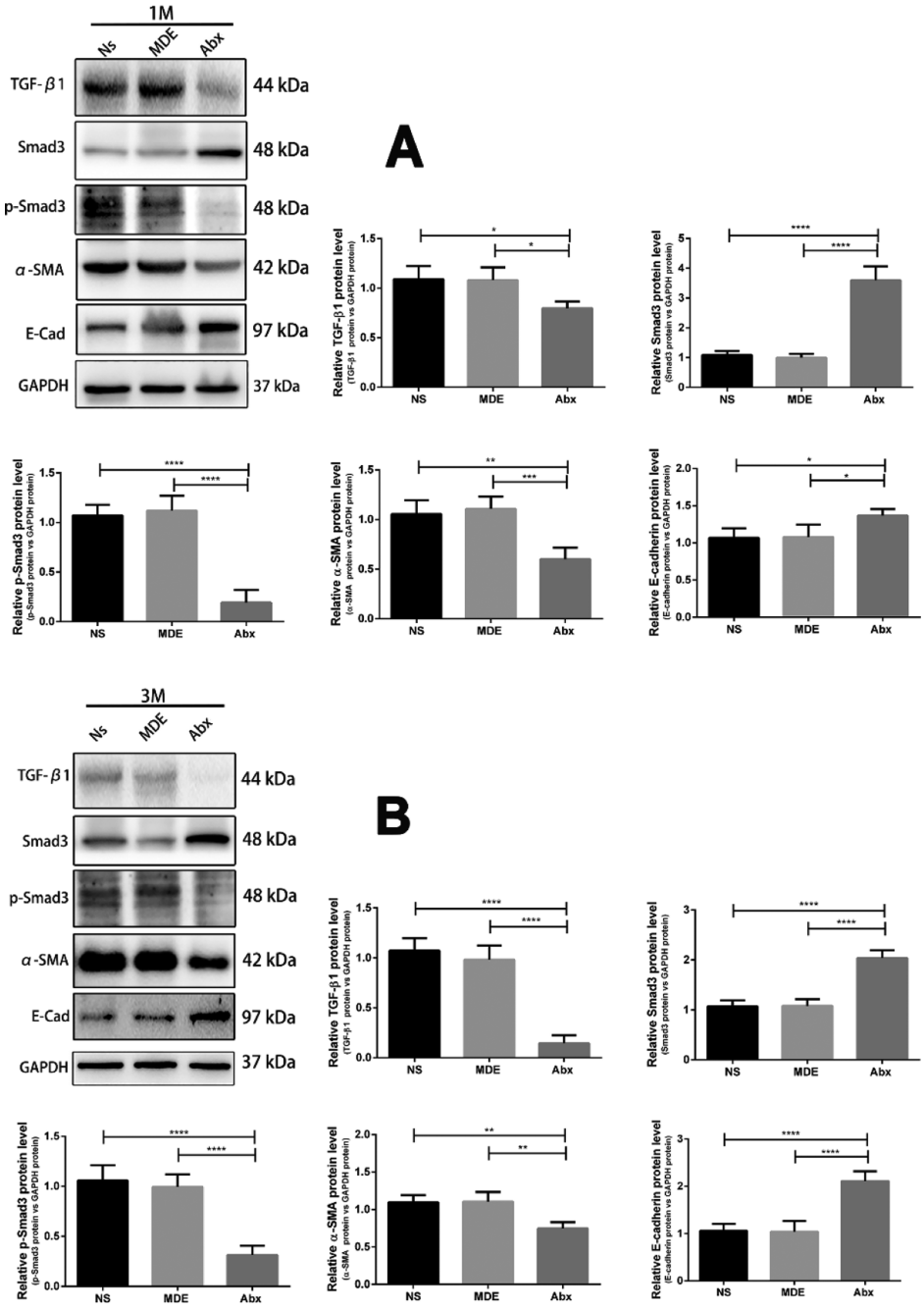

Figure 9. Antibiotic pretreatment regulates the TGF-β1/Smad-3/α-SMA/E-cadherin signaling pathway in the ileum of mice. (A) Protein expression of TGF-β1, Smad-3, α-SMA, and E-cadherin in the ileum of mice 1 month after radiation. (B) Protein expression of TGF-β1, Smad-3, α-SMA, and E-cadherin in the ileum of mice 3 months after radiation. The results were expressed as mean ± SEM. n = 3.*P < 0.05, **P < 0.01, ***P < 0.001, ****P < 0.0001.

Abx pretreatment can significantly increase the reconstitution of gut microbiota after radiation in mice. Furthermore, Abx pretreatment alleviated radiation-induced intestinal damage by regulating the LPS/TLR4/MyD88/NF-κB p65/macrophage polarization/TGF-β1/Smad-3 signaling pathway and ultimately improved viability of mice.

In the present study, we used 16S rRNA sequencing technology to compare the composition of the gut microbiota of mice before and after radiation. Our data showed that abdominal radiation caused gut microbiota disorder and at the same time caused a decrease in the diversity of intestinal microbiota in mice, which was consistent with the sequencing results of intestinal microbiota in patients with clinical radiation-induced intestinal diseases.[18] In addition, abdominal radiation can result in an increase in several intestinal pathogens. *Proteobacteria* contains abundant pathogenic bacteria, which are low in healthy mice.[19] This study found that the abundance of *proteobacteria* was significantly increased after radiation (from 7.4 to 22.0%). Meanwhile, the abundance of *Verrucomicrobia* was decreased from 2.9 to 0.0006% after radiation. A recent study has shown that *Verrucomicrobia* may have potential anti-inflammatory properties.[20] The reduction of *Verrucomicrobia* abundance in our study indicated that mice after abdominal radiation may be more susceptible to

https://dx.doi.org/10.1021/acsomega.9b03906
ACS Omega 2020, 5, 2967−2977

inflammatory reactions. A previous study demonstrated that radiation-induced intestinal damage leads to changes in the metabolomics of the intestine in mice, reducing short-chain fatty acids, including acetate, propionate, and butyrate.[21] Therefore, we speculate that the change in the intestinal microenvironment promoted or inhibited the colonization of certain specific bacteria, leading to reduction of the gut microbiota diversity. Excessive proliferation of pathogenic bacteria may induce bacteremia and impairment of post-radiation intestinal mucosal repair, eventually leading to unfavorable prognosis of radiation enteropathy.

Previous studies have found that sterile mice under the same dose of radiation have minor epithelial cell damage than specific-pathogen-free (SPF) mice.[14] This study suggested that the gut microbiota played an important role in intestinal radiation damage. Thus, we first performed different antibiotic pretreatments on mice to clear their intestinal microbiota. Our findings showed that the Abx pretreatment could effectively remove most of the intestinal microbiota in the feces of mice, simulating the intestinal environment of sterile mice. However, the pretreatment of MDE could only remove some intestinal bacteria and aggravate intestinal microbiota disorder in mice. We further studied the effects of antibiotic pretreatment on the remodeling ability of intestinal microbiota at 3 months after radiation. Our data suggested that the antibiotic pretreatment groups had more special OTUs than the control group. In addition, compared with the control group, the relative abundance of *Verrucomicrobia* in the Abx pretreatment group was markedly increased. The reconstitution effect of MDE pretreatment on intestinal microbiota after radiation was also superior to that of the control group, and the relative abundance of *Verrucomicrobia* was also improved. Taken together, Abx pretreatment enhanced the reconstitution ability of intestinal microbiota after radiation, and the intestinal microbiota diversity was better than that of the control group. Although pretreatment with MDE aggravated the intestinal microbiota disorder in mice, it also improved the ability of the intestinal microbiota reconstitution after radiation-induced intestinal injury, and the diversity of the reconstructed intestinal microbiota was more abundant.

In addition to disrupting the structure and composition of the gut microbiota, abdominal radiation can also induce intestinal inflammation and mucosal barrier dysfunction.[22−24] Our results revealed that the mortality rate of mice in Ns and MDE pretreatment groups after abdominal radiation is higher, and the pretreatment of Abx could significantly improve the survival rate of mice after radiation. Moreover, protein expression of PCNA and cleaved caspase3 showed that the intestinal epithelial cells of Abx pretreatment group mice had stronger proliferative ability and apoptosis ability at 1 month and 3 months after radiation. Apoptosis refers to the orderly death of cells that are controlled by genes to maintain homeostasis. Apoptosis is not a phenomenon of autologous injury under pathological conditions, but a death process that is actively pursued to better adapt to the living environment.[25] The increase in apoptosis and cell proliferation at 1 and 3 months after radiation indicated that Abx pretreatment contributed to intestinal epithelial cell recovery and regeneration. Studies have shown that the presence of a large number of bacteria in the gut may enter the bloodstream when the intestinal mucosal barrier is impaired, leading to bacteremia and toxemia, thereby aggravating intestinal wall damage and leading to systemic inflammatory response and increased mortality.[26,27] In this study, compared with the control group (Ns group), the content of LPS in the ileum was significantly reduced in the Abx-pretreated mice. A previous study demonstrated that TLR4 antagonist C34 pretreatment reduces radiation-induced cell damage and death in mice.[28] Consistently, our study revealed that the protein abundance of TLR4 in the ileum was significantly reduced in the ileum of Abx-pretreated mice. Furthermore, the protein expression of MyD88 and phosphorylated NF-κB p65 was also inhibited in the Abx pretreatment group. A recent study suggested that the macrophage migration inhibitory factor serves a pivotal role in the regulation of radiation-induced cardiac senescence.[29] In the present study, the protein expression of M1 macrophage marker iNOS and M2 macrophage marker CD163 in the ileum of the Abx pretreatment group was significantly lower than that of the control group. The increase in macrophage populations in the lamina propria of the gut is thought to be involved in fibrosis of the intestine, and macrophage-secreting cytokines such as TGF-β1 could drive the deposition and fibrosis of fibroblasts and extracellular matrices.[30] At week 26 after radiation, TGF-β1 in fibroblasts in lamina propria, endothelial cells, and smooth muscle remained at a high level.[31] Our findings showed that Abx pretreatment inhibits the protein abundance of TGF-β1, phosphorylated Smad-3, and α-SMA, suggesting that Abx could reduce intestinal wall fibrosis by downregulating TGF-β1/Smad-3 signaling pathways in radiated mice.

In summary, we report herein that abdominal radiation causes intestinal microecological disturbances, reduces microbe diversity, and increases the relative abundance of pathogenic bacteria such as *Proteobacteria* in mice. Abx and MDE pretreatment are conducive to reconstitute the intestinal microbiota of radiated mice. Furthermore, Abx pretreatment alleviates intestinal damage by regulating LPS/TLR4/MyD88/NF-κB p65/macrophage polarization/TGF-β1/Smad-3 signaling pathways, ultimately improving the viability of mice with postradiation intestinal damage. Thus, our findings provide a potential therapy for mammals at risk of abdominal radiation-induced intestinal damage.

MATERIALS AND METHODS

Animal and Experimental Design. Male C57BL/6 mice aged 8−10 weeks were purchased from the Institute of Model Animals of Nanjing University and entrusted to the Department of Comparative Medicine of Jinling Hospital for breeding and management. All experimental mice were housed in the SPF environment, maintained at constant temperature and humidity, maintained for 12 h light/dark cycle, free eating and drinking, and fed adaptively for at least 1 week before the experiment. The use and operation of laboratory animals are in accordance with the "Guidelines for the Protection and Application of Laboratory Animals" issued by the National Institutes of Health (NIH Publication no. 85-23, 1996 version) and the corresponding regulations of the Animal Management Committee of Jinling Hospital (JH-20180714).

Antibiotic Pretreatment Program. In order to simulate the sterile condition, we performed antibiotic pretreatment on the mice. Mice were divided into the normal saline group (Ns group or Con group), MDE group, and Abx group. The MDE group had a MDE concentration of 1 g/L; the Abx treatment group consisted of MDE 1 g/L, vancomycin 0.5 g/L, ampicillin 1 g/L, and gentamicin 1 g/L. The mice were intragastrically

https://dx.doi.org/10.1021/acsomega.9b03906
ACS Omega 2020, 5, 2967−2977

administered once a day, 0.4 mL each time, for a total of 14 days.

Abdominal Radiation Program. After intragastric administration for 14 days, C57BL/6 mice were anesthetized with an appropriate amount of pentobarbital (1%, 35 mg/kg). After the mice were anesthetized, the mice were fixed on cardboard. The mice were then subjected to a local high-dose abdominal precision radiation (225 kV/17 mA Cs137 linear accelerator with a dose rate of 2 Gy/min*5 min and a single dose of 10 Gy). Radiation range: concentrated in the two-leg connection level to the above 2 cm area, and the rest of the body was shielded with a 5 cm lead.

Sample Collection. The mice were sacrificed by cervical dislocation. The abdominal cavity was opened by midline incision, the terminal ileum and cecum of the mouse were cut with sterile scissors, and the feces of the terminal ileum and cecum were inhaled into a 1.5 mL enzyme-free sterile tube, each about 200 mg, at 14 days after intragastrical administration (Pre groups, including the Pre.Con14 group, Pre.MDE14, and Pre.Abx14 group) and 3 months after radiation (Post groups, including the Post.Con14 group, Post.MDE14, and Post.Abx14 group). In addition, a segment of the ileum from the same position of each animal was collected immediately and washed three times in ice-cold PBS buffer. The tissue samples were frozen immediately in liquid nitrogen or fixed in 4% buffered paraformaldehyde.

Protein Extraction and Western Blot Analysis. Total protein was extracted using basic lysis buffer. The protein concentration was measured using a Pierce BCA Protein Assay Kit (Pierce, Rockford, IL, USA). After the proteins had been denatured by boiling for 5 min, they were separated by electrophoresis in SDS-PAGE and transferred onto a nitrocellulose membrane (BioTrace; Pall Corp., USA). The membrane was blocked with 5% BSA for 1 h and then incubated overnight at 4 °C with the specific primary antibodies. After several washes in Tris-buffered saline with Tween, membranes were incubated with secondary antibodies for 2 h at room temperature. After several washes, bands were detected by enhanced chemiluminescence using the LumiGlo substrate (Super Signal West Pico; Pierce, USA), and the signals were recorded by an imaging system (Bio-Rad, USA) and analyzed with Quantity One software (Bio-Rad, USA). GAPDH was used as a loading control in the western blot. Protein abundance was expressed as the fold change relative to the mean value of the control group. Information about the antibodies is shown in Table 1.

LPS Assay. The LPS content in ileum tissue was measured by LPS enzyme-linked immunosorbent assay kits (CSB-E13066m, CUSABIO). The procedures were performed according to the manufacturer's instructions.

HE, Mason, Sirius Red, TUNEL, and Ki67 Staining. Specimens of the ileum were prepared for histological examination by fixing in 4% polyformaldehyde-buffered solution, embedding in paraffin, and sectioning. Specimens were examined for injury after hematoxylin and eosin staining as described by a previous study.[32]

For Masson staining, the sections were placed in Gill-modified hematoxylin staining solution for 5−10 min and rinsed with deionized water. Then, place the sections in the hydrochloric acid alcohol differentiation solution for several tens of seconds and rinse for several minutes with running water. They were stained with Masson complex staining solution for 5−10 min, slightly washed with deionized water, treated with 1% phosphotungstic acid solution for about 5 min, and aniline blue was used as a counterstain for 5 min and treated with 1% glacial acetic acid for 1 min. It is dehydrated by 95% alcohol, dehydrated with anhydrous ethanol, transparent with xylene, and sealed with neutral gum.

For Sirius red staining, the sections were stained with Sirius Red staining for 1 h. They were rinsed with deionized water to remove excess staining from the surface of the section. It is conventionally dehydrated, transparent, and covered with a neutral gum. It is naturally dried, stored at room temperature, and placed under an ordinary light microscope for observation.

Apoptotic epithelial cells in the ileum were analyzed using the terminal deoxynucleotidyl transferase (TdT)-mediated dUTP-biotin nick end labeling (TUNEL) assay according to the manufacturer's instruction. TUNEL-positive nuclei were clearly identified as brown-stained nuclei, which indicated the presence of DNA fragmentation because of apoptosis. TUNEL-positive cells were determined by observing 1000 cells in randomly selected fields.

DNA Extraction, 16S rRNA Gene Amplification, and Sequencing. Total DNA was extracted from 200 mg of each fecal specimen using the QIAamp R Fast DNA Stool Mini Kit (Qiagen Ltd., Germany) in accordance with manufacturer's instructions. The V4 region of the 16S rRNA gene was amplified with universal primers 515F (GTGCCAGCMGCCGCGGTAA) and 806R (GGACTACHVGGGTWTCTAAT), as described by a previous study.[33] The amplified products were detected using agarose gel electrophoresis (2% agarose), recovered using an AxyPrep DNA Gel Recovery Kit (Axygen Biosciences, Union City, CA, United States), and then quantified using Qubit 2.0 Fluorometer (Thermo Fisher Scientific, Waltham, MA, United States) to pool into equimolar amounts. Amplicon libraries were sequenced on the Illumina MiSeq 2500 platform (Illumina, San Diego, CA, United States) for paired-end reads of 250 bp.

Analysis of Sequencing Data. The raw paired-end reads were assembled into longer sequences and quality-filtered using PANDAseq (version 2.9) to remove the low-quality reads with a length of <220 nucleotides (nt) or >500 nt, an average quality score of <20, and sequences containing >3 nitrogenous bases.[34] The high-quality sequences were clustered into OTUs with a 97% similarity using UPARSE (version 7.0)[35] in QIIME (version 1.8),[36] and the chimeric sequences were removed using UCHIME.[37] Taxonomy was assigned to OTUs using the RDP classifier[38] against the SILVA

Table 1. Antibodies Used in the Present Study

antibody	introduction and company	dilution ratio
PCNA	#2586, Cell Signaling Technology	1:1000
cleaved caspase3	ab184787, Abcam	1:1000
TLR4	sc-293072, Santa Cruz	1:200
MyD88	#AB32107, AbSci	1:2000
Phospho-NF-kB p65	#3033, Cell Signaling Technology	1:1000
iNOS	ab178945, Abcam	1:1000
CD163	ab182422, Abcam	1:1000
TGF-β1	ab92486, Abcam	1:1000
Smad3	ab40854, Abcam	1:1000
phospho-Smad3	ab52903, Abcam	1:1000
α-SMA	ab18147, Abcam	1:1000
E-cadherin	ab76055, Abcam	1:1000
GAPDH	ap0066, Bioworld	1:10,000

https://dx.doi.org/10.1021/acsomega.9b03906
ACS Omega 2020, 5, 2967−2977

16S rRNA gene database,[39] with a confidence threshold of 70%.

The observed species, Chao index, and Simpson diversity index per sample were calculated by the MOTHUR program (version v.1.30.1).[40] Heat maps were generated with the "vegan" package in R (version 3.3.1). PCA was performed based on Bray−Curtis distances using QIIME (version 1.8).

Statistical Analysis. Data were presented as means ± SD. The numbers of replicates used for statistics are noted in the figures. The difference in the alpha-diversity was tested using Dunnett's *t*-test (SPSS 20.0). To determine differences between groups at a single time point, data were tested using 1-way ANOVA followed by Tukey's multiple comparisons test. The corrected *P*-values below 0.05 were regarded as statistically significant. Postradiation survival was estimated using the Kaplan−Meier method and compared using the log-rank test.

■ ASSOCIATED CONTENT

Supporting Information

The Supporting Information is available free of charge at https://pubs.acs.org/doi/10.1021/acsomega.9b03906.

Graph of histomorphology and immunohistochemistry (PDF)

■ AUTHOR INFORMATION

Corresponding Authors

Guoyi Shao − *Department of General Surgery, The Affiliated Jiangyin Hospital of Southeast University Medical College, Wuxi, Jiangsu 214400, China;* orcid.org/0000-0003-0126-5089; Email: shaoguoyi666@163.com

Shuanghai Liu − *Department of General Surgery, The Affiliated Jiangyin Hospital of Southeast University Medical College, Wuxi, Jiangsu 214400, China*; Email: shuanghailiu@126.com

Authors

Zhenguo Zhao − *Department of General Surgery, The Affiliated Jiangyin Hospital of Southeast University Medical College, Wuxi, Jiangsu 214400, China*

Wei Cheng − *Department of General Surgery, Jiangsu Province Hospital of Chinese Medicine, Affiliated Hospital of Nanjing University of Chinese Medicine, Nanjing 210029, China*

Wei Qu − *Department of Pharmacy, The Affiliated Jiangyin Hospital of Southeast University Medical College, Wuxi, Jiangsu 214400, China*

Complete contact information is available at: https://pubs.acs.org/10.1021/acsomega.9b03906

Author Contributions

Z.Z. and W.C. contributed equally. Z.Z. and W.C. performed the experiments and drafted the manuscript; W.Q. performed the experiments and analyzed the data; G.S. and S.L. contributed to the experimental design and revised the manuscript; and G.S. and S.L conceived the ideas, designed the experiments, and finalized the manuscript. All authors read and approved the final manuscript.

Notes

The authors declare no competing financial interest.

■ ACKNOWLEDGMENTS

This work was financially supported by Wuxi Health and Family Planning Commission Youth Research Foundation (no. Q201720) and Li Jie-shou Gut Barrier Foundation (no. LJS-201708).

■ ABBREVIATIONS

Abx, antibiotic cocktail; MDE, metronidazole; ROS, reactive oxygen species; NOS, reactive nitrogen species; SPF, specific-pathogen-free; H&E, hematoxylin and eosin

■ REFERENCES

(1) Abayomi, J.; Kirwan, J.; Hackett, A. The prevalence of chronic radiation enteritis following radiotherapy for cervical or endometrial cancer and its impact on quality of life. *Eur. J. Oncol. Nurs.* **2009**, *13*, 262−267.

(2) DeCosse, J. J.; Rhodes, R. S.; Wentz, W. B.; Reagan, J. W.; Dworken, H. J.; Holden, W. D. The natural history and management of radiation induced injury of the gastrointestinal tract. *Ann. Surg.* **1969**, *170*, 369−384.

(3) Andreyev, J. Gastrointestinal complications of pelvic radiotherapy: are they of any importance? *Gut* **2005**, *54*, 1051−1054.

(4) Ward, J. F. DNA damage produced by ionizing radiation in mammalian cells: identities, mechanisms of formation, and reparability. *Prog. Nucleic Acid Res. Mol. Biol.* **1988**, *35*, 95−125.

(5) Turrens, J. F. Mitochondrial formation of reactive oxygen species. *J. Physiol.* **2003**, *552*, 335−344.

(6) Mikkelsen, R. B.; Wardman, P. Biological chemistry of reactive oxygen and nitrogen and radiation-induced signal transduction mechanisms. *Oncogene* **2003**, *22*, 5734−5754.

(7) Banerjee, S.; Aykin-Burns, N.; Krager, K. J.; Shah, S. K.; Melnyk, S. B.; Hauer-Jensen, M.; Pawar, S. A. Loss of C/EBPδ enhances IR-induced cell death by promoting oxidative stress and mitochondrial dysfunction. *Free Radic. Biol. Med.* **2016**, *99*, 296−307.

(8) Bergonie, J.; Tribondeau, L. Interpretation of some results from radiotherapy and an attempt to determine a rational treatment technique. 1906. *Yale J. Biol. Med.* **2003**, *76*, 181−182.

(9) Darwich, A. S.; Aslam, U.; Ashcroft, D. M.; Rostami-Hodjegan, A. Meta-analysis of the turnover of intestinal epithelia in preclinical animal species and humans. *Drug Metab. Dispos.* **2014**, *42*, 2016−2022.

(10) Nejdfors, P.; Ekelund, M.; Weström, B. R.; Willén, R.; Jeppsson, B. Intestinal permeability in humans is increased after radiation therapy. *Dis. Colon Rectum* **2000**, *43*, 1582−1587. ; discussion 1587-8

(11) Shukla, P. K.; Gangwar, R.; Manda, B.; Meena, A. S.; Yadav, N.; Szabo, E.; Balogh, A.; Lee, S. C.; Tigyi, G.; Rao, R. Rapid disruption of intestinal epithelial tight junction and barrier dysfunction by ionizing radiation in mouse colon in vivo: protection by N-acetyl-l-cysteine. *Am. J. Physiol. Gastrointest. Liver Physiol.* **2016**, *310*, G705−G715.

(12) Reis Ferreira, M.; Andreyev, H. J. N.; Mohammed, K.; Truelove, L.; Gowan, S. M.; Li, J.; Gulliford, S. L.; Marchesi, J. R.; Dearnaley, D. P. Microbiota- and Radiotherapy-Induced Gastrointestinal Side-Effects (MARS) Study: A Large Pilot Study of the Microbiome in Acute and Late-Radiation Enteropathy. *Clin. Cancer Res.* **2019**, *25*, 6487−6500.

(13) Liu, X.; Zhou, Y.; Wang, S.; Guan, H.; Hu, S.; Huang, R.; Zhou, P. Impact of Low-dose Ionising Radiation on the Composition of the Gut Microbiota of Mice. *Toxicol. Sci.* **2019**, *171*, 258.

(14) Crawford, P. A.; Gordon, J. I. From The Cover: Microbial regulation of intestinal radiosensitivity. *Proc. Natl. Acad. Sci. U.S A.* **2005**, *102*, 13254−13259.

(15) Abayomi, J.; Kirwan, J.; Hackett, A.; Bagnall, G. A study to investigate women's experiences of radiation enteritis following radiotherapy for cervical cancer. *J. Hum. Nutr. Diet.* **2005**, *18*, 353−363.

(16) Hauer-Jensen, M.; Denham, J. W.; Andreyev, H. J. N. Radiation enteropathy–pathogenesis, treatment and prevention. *Nat. Rev. Gastroenterol. Hepatol.* **2014**, *11*, 470−479.

(17) Hauer-Jensen, M.; Wang, J.; Denham, J. W. Bowel injury: current and evolving management strategies. *Semin. Radiat. Oncol.* **2003**, *13*, 357−371.
(18) Nam, Y.-D.; Kim, H. J.; Seo, J.-G.; Kang, S. W.; Bae, J.-W. Impact of Pelvic Radiotherapy on Gut Microbiota of Gynecological Cancer Patients Revealed by Massive Pyrosequencing. *PLoS One* **2013**, *8*, No. e82659.
(19) Human Microbiome Project Consortium. Structure, function and diversity of the healthy human microbiome. *Nature* **2012**, *486*, 207−214.
(20) Derrien, M.; Belzer, C.; de Vos, W. M. Akkermansia muciniphila and its role in regulating host functions. *Microb. Pathog.* **2017**, *106*, 171−181.
(21) Yang, J.; Ding, C.; Dai, X.; Lv, T.; Xie, T.; Zhang, T.; Gao, W.; Gong, J.; Zhu, W.; Li, N. Soluble Dietary Fiber Ameliorates Radiation-Induced Intestinal Epithelial-to-Mesenchymal Transition and Fibrosis. *JPEN, J. Parenter. Enteral Nutr.* **2017**, *41*, 1399.
(22) Hovdenak, N.; Wang, J.; Sung, C.-C.; Kelly, T.; Fajardo, L. F.; Hauer-Jensen, M. Clinical significance of increased gelatinolytic activity in the rectal mucosa during external beam radiation therapy of prostate cancer. *Int. J. Radiat. Oncol., Biol., Phys.* **2002**, *53*, 919−927.
(23) François, A.; Milliat, F.; Guipaud, O.; Benderitter, M. Inflammation and immunity in radiation damage to the gut mucosa. *BioMed Res. Int.* **2013**, *2013*, 1.
(24) Paris, F.; Fuks, Z.; Kang, A.; Capodieci, P.; Juan, G.; Ehleiter, D.; Haimovitz-Friedman, A.; Cordon-Cardo, C.; Kolesnick, R. Endothelial apoptosis as the primary lesion initiating intestinal radiation damage in mice. *Science* **2001**, *293*, 293−297.
(25) Elmore, S. Apoptosis: a review of programmed cell death. *Toxicol. Pathol.* **2007**, *35*, 495−516.
(26) Flannigan, K. L.; Taylor, M. R.; Pereira, S. K.; Rodriguez-Arguello, J.; Moffat, A. W.; Alston, L.; Wang, X.; Poon, K. K.; Beck, P. L.; Rioux, K. P.; Jonnalagadda, M.; Chelikani, P. K.; Galipeau, H. J.; Lewis, I. A.; Workentine, M. L.; Greenway, S. C.; Hirota, S. A. An intact microbiota is required for the gastrointestinal toxicity of the immunosuppressant mycophenolate mofetil. *J. Heart Lung Transplant.* **2018**, *37*, 1047.
(27) Gäbele, E.; Dostert, K.; Hofmann, C.; Wiest, R.; Schölmerich, J.; Hellerbrand, C.; Obermeier, F. DSS induced colitis increases portal LPS levels and enhances hepatic inflammation and fibrogenesis in experimental NASH. *J. Hepatol.* **2011**, *55*, 1391−1399.
(28) Lam, V.; Moulder, J. E.; Salzman, N. H.; Dubinsky, E. A.; Andersen, G. L.; Baker, J. E. Intestinal microbiota as novel biomarkers of prior radiation exposure. *Radiat. Res.* **2012**, *177*, 573−583.
(29) Hu, Y.; Xia, W.; Hou, M. Macrophage migration inhibitory factor serves a pivotal role in the regulation of radiation-induced cardiac senescencethrough rebalancing the microRNA-34a/sirtuin 1 signaling pathway. *Int. J. Mol. Med.* **2018**, *42*, 2849−2858.
(30) Rieder, F.; Brenmoehl, J.; Leeb, S.; Scholmerich, J.; Rogler, G. Wound healing and fibrosis in intestinal disease. *Gut* **2007**, *56*, 130−139.
(31) Wang, J.; Zheng, H.; Sung, C.-C.; Richter, K. K.; Hauer-Jensen, M. Cellular sources of transforming growth factor-beta isoforms in early and chronic radiation enteropathy. *Am. J. Pathol.* **1998**, *153*, 1531−1540.
(32) Tao, S.; Duanmu, Y.; Dong, H.; Tian, J.; Ni, Y.; Zhao, R. A high-concentrate diet induced colonic epithelial barrier disruption is associated with the activating of cell apoptosis in lactating goats. *BMC Vet. Res.* **2014**, *10*, 235.
(33) Hong, X.; Chen, J.; Liu, L.; Wu, H.; Tan, H.; Xie, G.; Xu, Q.; Zou, H.; Yu, W.; Wang, L.; Qin, N. Metagenomic sequencing reveals the relationship between microbiota composition and quality of Chinese Rice Wine. *Sci. Rep.* **2016**, *6*, 1.
(34) Masella, A. P.; Bartram, A. K.; Truszkowski, J. M.; Brown, D. G.; Neufeld, J. D. PANDAseq: paired-end assembler for illumina sequences. *BMC Bioinf.* **2012**, *13*, 31.
(35) Edgar, R. C. UPARSE: highly accurate OTU sequences from microbial amplicon reads. *Nat. Methods* **2013**, *10*, 996−998.
(36) Caporaso, J. G.; Kuczynski, J.; Stombaugh, J.; Bittinger, K.; Bushman, F. D.; Costello, E. K.; Fierer, N.; Peña, A. G.; Goodrich, J. K.; Gordon, J. I.; Huttley, G. A.; Kelley, S. T.; Knights, D.; Koenig, J. E.; Ley, R. E.; Lozupone, C. A.; McDonald, D.; Muegge, B. D.; Pirrung, M.; Reeder, J.; Sevinsky, J. R.; Turnbaugh, P. J.; Walters, W. A.; Widmann, J.; Yatsunenko, T.; Zaneveld, J.; Knight, R. QIIME allows analysis of high-throughput community sequencing data. *Nat. Methods* **2010**, *7*, 335−336.
(37) Edgar, R. C.; Haas, B. J.; Clemente, J. C.; Quince, C.; Knight, R. UCHIME improves sensitivity and speed of chimera detection. *Bioinformatics* **2011**, *27*, 2194−2200.
(38) Bacci, G.; Bani, A.; Bazzicalupo, M.; Ceccherini, M. T.; Galardini, M.; Nannipieri, P.; Pietramellara, G.; Mengoni, A. Evaluation of the Performances of Ribosomal Database Project (RDP) Classifier for Taxonomic Assignment of 16S rRNA Metabarcoding Sequences Generated from Illumina-Solexa NGS. *J. Genom.* **2015**, *3*, 36−39.
(39) Pruesse, E.; Quast, C.; Knittel, K.; Fuchs, B. M.; Ludwig, W.; Peplies, J.; Glockner, F. O. SILVA: a comprehensive online resource for quality checked and aligned ribosomal RNA sequence data compatible with ARB. *Nucleic Acids Res.* **2007**, *35*, 7188−7196.
(40) Schloss, P. D.; Westcott, S. L.; Ryabin, T.; Hall, J. R.; Hartmann, M.; Hollister, E. B.; Lesniewski, R. A.; Oakley, B. B.; Parks, D. H.; Robinson, C. J.; Sahl, J. W.; Stres, B.; Thallinger, G. G.; Van Horn, D. J.; Weber, C. F. Introducing mothur: open-source, platform-independent, community-supported software for describing and comparing microbial communities. *Appl. Environ. Microbiol.* **2009**, *75*, 7537−7541.

https://dx.doi.org/10.1021/acsomega.9b03906
ACS Omega 2020, 5, 2967−2977